

**Focal Hepatic Tumors Using Inversion Recovery
Sequence of 0.1-T MRI**
— Basic and Clinical Evaluation by Gray Scale vs T1 Values —

Hisato HOMMA¹, Naoaki SHINTANI², Ehichi MASUKO²,
Naoki WATANABE², Yutaka KOHGO², Shigeyuki IKEDA¹,
Takashi BETSUYAKU³ and Yoshiro NIITSU²

¹ *Division of Gastroenterology, National Sapporo Hospital,
Hokkaido Cancer Center, Kikusui 4-2, Shiroishiku, Sapporo 003, Japan*

² *Department of internal Medicine (Section 4), Sapporo Medical
College, South 1, West 16, Chuo-ku, Sapporo 060, Japan*

³ *Department of internal Medicine, National Noboribetsu Hospital,
Onsenchou 5, Noboribetsu, Noboribetsu 059-05, Japan*

ABSTRACT

Optimum conditions for image quality contrast were studied with phantom method by means of MRI system (of constant conduction type; 0.1-T) in order to detect tumor lesions of liver that show no distinct contrast by usual roentgenographic methods.

Signal intensity of liver, fat and muscle were maximally suppressed at 1000 ms of TR and 100 ms of TI by the short inversion time inversion recovery (STIR) method, resulting in distinct visualization of liver tumor with extremely good contrast. Clinical investigation with the usual T1- and T2- weighted images under the same conditions identified hepatocellular carcinoma in 22 out of 31 patients (37 of 58 nodules, 64%), cholangiocellular carcinoma 3 of 5 (3 of 6 nodules, 50%), metastatic liver cancer in 55 out of 68 (111 of 143 nodules, 78%), hepatic hemangioma in 32 out of 36 (41 of 47 nodules, 87%) and liver cyst in 8 out of 8 (100%). In contrast, hepatocellular carcinoma was visualized in 30 out of 31 patients (54 of 58 nodules, 93%), cholangiocellular carcinoma in 5 out of 5 (6 of 6 nodules, 100%), metastatic liver cancer in 66 out of 68 (139 of 143 nodules, 97%), hepatic hemangioma in 36 out of 36 (47 of 47 nodules, 100%) and liver cyst in 8 out of 8 (100%).

The results suggest that STIR (TR: 1000 ms, TI: 100 ms, TE: 18 ms) is extremely useful in screening tumor lesions of the liver.

Key words: MRI, STIR, Focal hepatic tumors, Gray scale, T1 values

INTRODUCTION

In recent years, magnetic resonance imaging (MRI) has rapidly become available for clinical diagnosis. With the advent of high-magnetic-field MRI, the focus of MRI usage is currently shifting from diagnosis of tumor to MR angiography and ^{31}P -MR spectroscopy, reflecting the rapid progress in technology. However, practical MRI application for use in general hospitals is currently low- and medium-magnetic-field MRI by means of regular conduction and a permanent magnet, taking into consideration the conditions necessary for placement, price of the apparatus and operational cost. The inversion recovery method^(1,6,7), one of the MRI pulse sequence, is used less frequently for diagnosis of lesions in the abdominal region than the spin echo (SE) method, because the IR method is associated with a low S/N ratio due to prolonged TR and requires considerable time for imaging. However, the short inversion time inversion recovery (STIR) method, which involves a short inversion time (TI), has been applied for diagnosis of various diseases since Bydder *et al.*^(2,3) reported several advantages of this method, including 1) a low signal intensity of fat, 2) a less marked motion artifact associated with respiratory movement and 3) a higher tumor contrast^(8,13,15).

In the present study, we investigated tumor lesions in the liver, which cannot be visualized with clear contrast by the usual methods (IR and SE), using the STIR method with a 0.1-T regular conduction MRI apparatus. Prior to clinical use, we also carried out a fundamental study in order to obtain the optimal conditions for picture quality contrast, using phantoms to examine the relation between the Gray scale (GS) and the T1 values.

MATERIALS AND METHODS

A 0.1-T regular conduction MRI apparatus, Mark-J (Asahikasei), was used. The phantoms used for evaluation of the picture quality were 6 polyethylene bottles having a cross-sectional area of $\phi 60 \times 60$ mm. Their T1 values were adjusted to 100 (P-1), 200 (P-2), 300 (P-3), 400 (P-4), 500 (P-5) and 1000 ms (P-6), using a solution containing 3.944, 1.84, 1.18, 0.84, 0.632 and 0.264 g/100 ml, respectively, of $\text{NiSO}_4 \cdot 6\text{H}_2\text{O}$ (Fig. 1).

As pulse sequences, the IR method (TR: 1000~1500 ms, TI: 500~900 ms, TE: 18 ms) was used for T1-weighted images (T1-WI), and the SE method (TR: 1800 ms, TE: 60~90 ms) for T2-WI. In addition, TR of 1000~1500 ms, TI of 50~300 ms and TE of 18 ms were used for the STIR method. The slice thickness was 5~10 mm, with a matrix of 256×256 pixels. The frequency counting was 2. The window width of pictures is constant.

The subjects were 144 patients comprising 31 with hepatocellular carcinoma

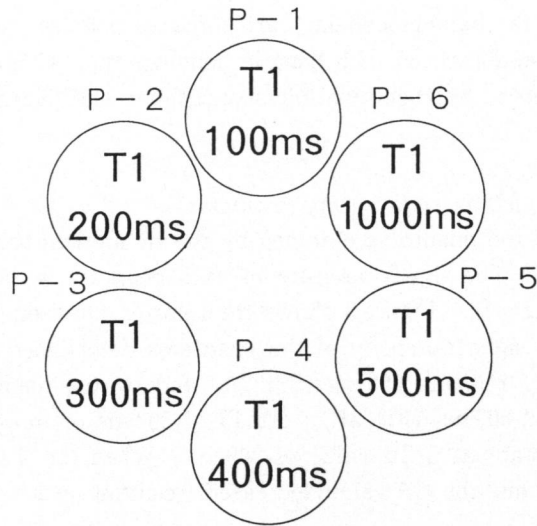


Fig. 1 The distribution of $\phi 60 \times 60$ mm phantoms.

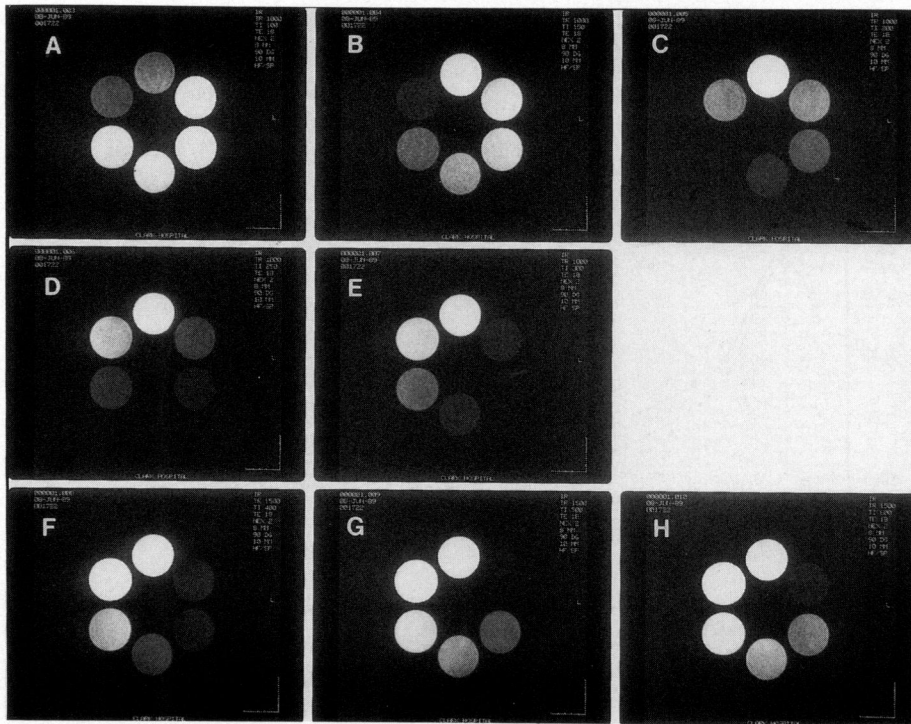


Fig. 2 The contrast of phantoms using IR method.

A : TI=100 ms, B : TI=150 ms, C : TI=200 ms, D : TI=250 ms,
 E : TI=300 ms, F : TI=400 ms, G : TI=500 ms, H : TI=1000 ms

(58 nodules), 5 with cholangiocellular carcinoma (6 nodules), 68 with metastatic liver cancer (143 nodules), 36 with hepatic hemangioma (47 nodules) and 8 with liver cyst as diagnosed by abdominal ultrasonography and liver biopsy.

RESULTS

1. Evaluation of picture quality using phantoms

MR images of the phantoms obtained by the IR method using various TI are shown in Figure 2. The signal intensity of each phantom with a given TI value varied in reaction to TI. Figure 3 shows the relation between TI and GS values obtained from the signal intensity of the phantoms determined by the long TIIR method with TI of 800 and 900 ms (Fig. 3A) and by the medium TIIR method with TI of 500 and 600 ms (Fig. 3B). At TI of 500 ms or more, the peak signal intensity was constant at a T1 value of 200 ms. When the T1 value was lower or higher than 200 ms, the GS value decreased, resulting in a low signal intensity on MRI.

Figure 4 shows the relation between T1 and GS values obtained from the signal intensity of the phantoms determined by the STIR method with the TI of 50, 100, 150, 200, 300 and 400 ms (Figs. 4A and 4B). When TI was 50 or 100 ms (Fig. 4A), the GS value became higher as the T1 value increased. However, at

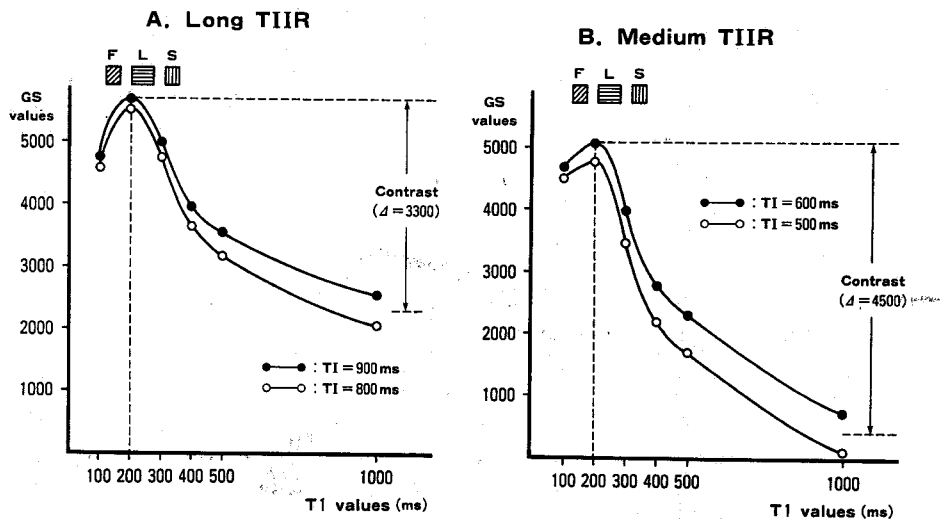


Fig. 3 The relation between T1 values and GS values obtained from the signal intensity of the phantoms determined by the IR method.

F : T1 value of healthy fat
 L : T1 value of healthy liver
 S : value of healthy spleen

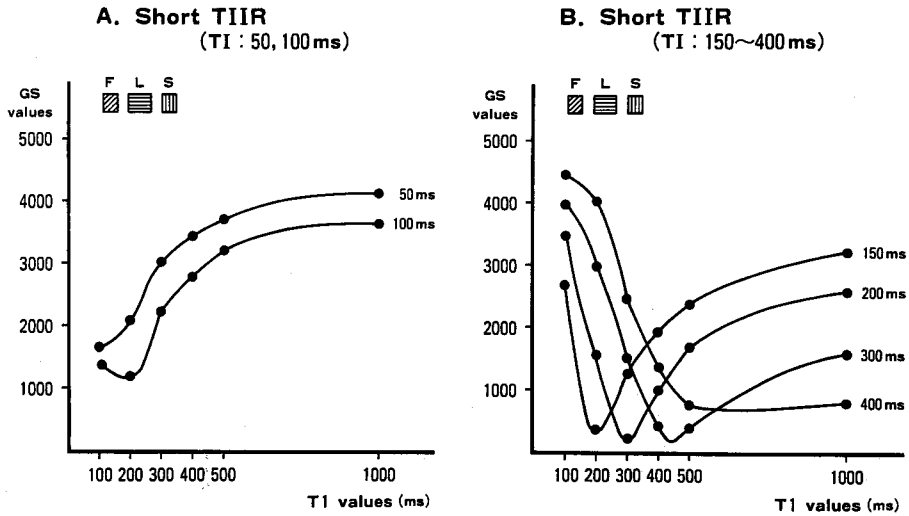


Fig. 4 The relation between T1 values and GS values obtained from the signal intensity of the phantoms determined by the IR methods.

F : T1 value of healty fat
 L : T1 value of healty liver
 S : T1 value of healty spleen

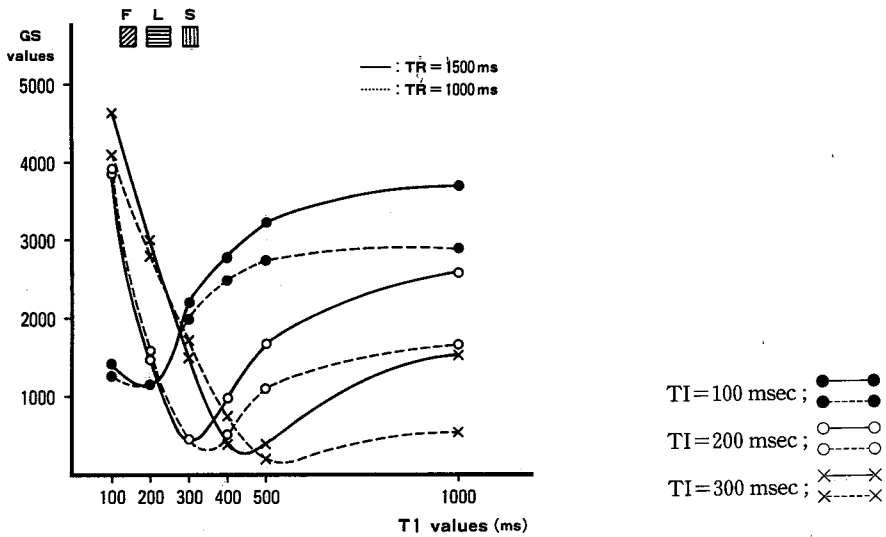


Fig. 5 The relation between T1 values and GS values determined by the IR method using TR as a parameter.

F : T1 value of healty fat
 L : T1 value of healty liver
 S : T1 value of healty spleen

TI of 150~400 ms (Fig. 4B), a certain T1 value which suppressed the signal intensity to the greatest extent was found for each TI. When the T1 value was lower or higher than this certain level, the GS value increased, resulting in a high signal on MRI.

The above analysis was focused on the relation between T1 and GS values, using TI as a parameter. In contrast, the relation between T1 and GS values determined by the STIR method (TI: 100, 200 and 300 ms) using TR as a parameter is shown in Figure 5. When T1 values were less than 400 ms, there were hardly any variations in GS with TR. On the other hand, when T1 values

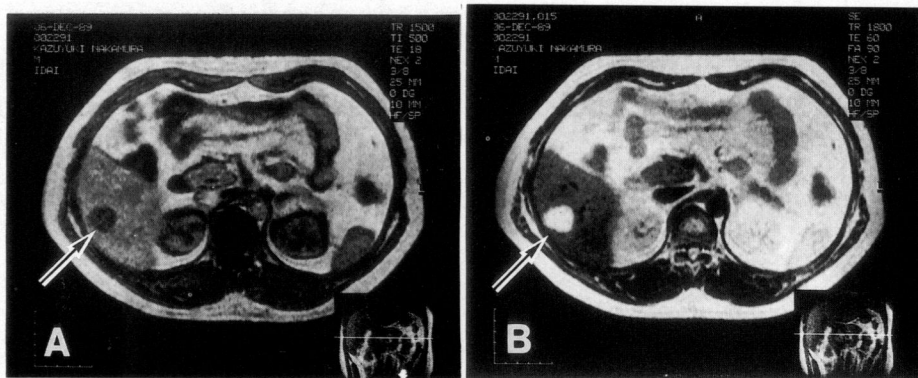


Fig. 6 MR imaging of hepatic hemangioma.

A. T1-weighted image by IR method (TR; 1500 ms, TI; 500 ms, TE; 18 ms)

B. T2-weighted image by SE method (TR; 1800 ms, TE; 60 ms)

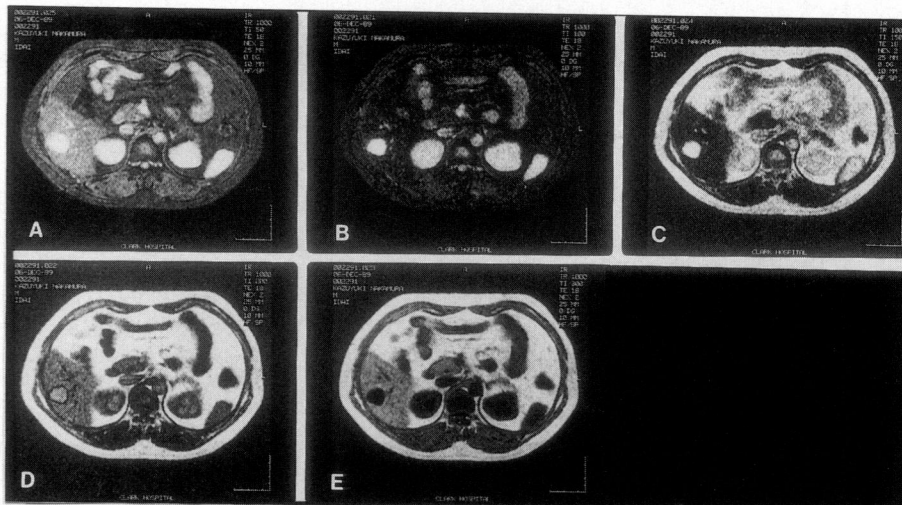


Fig. 7 MR imaging of hepatic hemangioma (Fig. 6) by STIR method.

A : TI=50 ms, B : TI=100 ms, C : TI=150 ms, D : TI=200 ms, E : TI=300 ms

were 400 ms or higher, GS decreased as TR decreased from 1500 ms to 1000 ms. This suggests that the contrast between the liver and the tumor, which has a higher T1 value, is greater at a TR of 1000 ms.

2. Examination of tumor lesions in the liver

Findings in a patient with hepatic hemangioma in S₆ are shown in Figure 6. The T2-WI (Fig. 6B) in the lower panel shows a higher signal in the tumor than in the partially observable spleen. This allows for diagnosis of hepatic hemangioma^(10,17). When the same area was examined by STIR, the signal intensity of tumor was high at a TI of 50~150 ms (Figs. 7A, 7B and 7C), equal at 200 ms (Fig. 7D) and low at 300 ms (Fig. 7E), respectively, in comparison with the signal intensity of the liver. In particular, when TI was 100 ms (Fig. 7B), the signal intensity of fat, liver and muscle were all suppressed, providing a clearly distinguishable image of the tumor.

Figure 8 shows a case of hepatocellular carcinoma in S₈. Although the

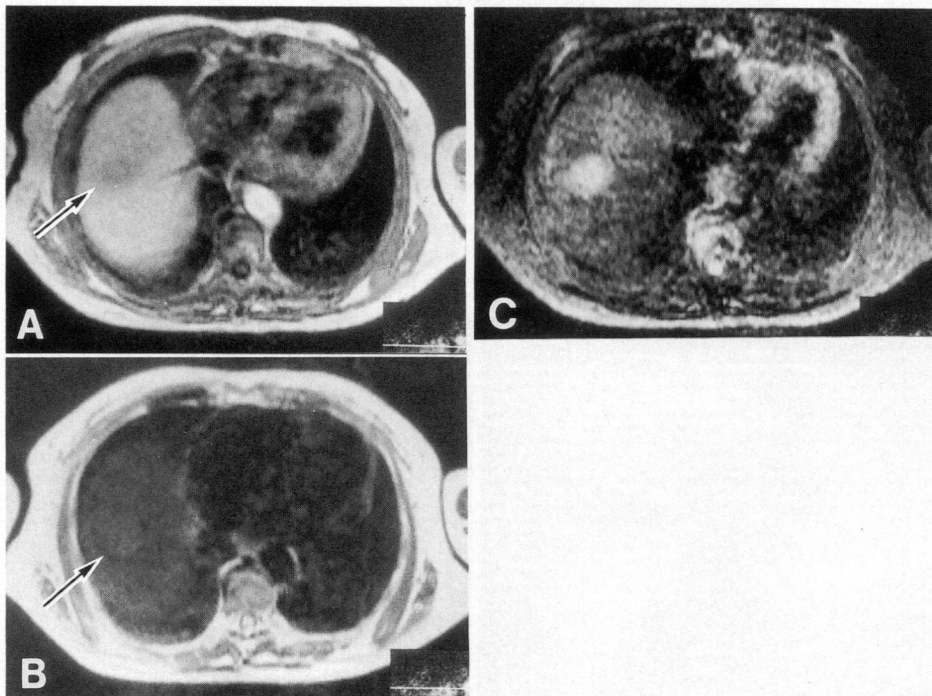


Fig. 8 MR imaging of primary hepatocellular carcinoma.

- A. T1-weighted image by IR method (TR; 1500 ms, TI; 500 ms, TE; 18 ms)
- B. T2-weighted image by SE method (TR; 1500 ms, TE; 60 ms)
- C. MR imaging of STIR method (TR; 1500 ms, TI; 100 ms, TE; 18 ms)

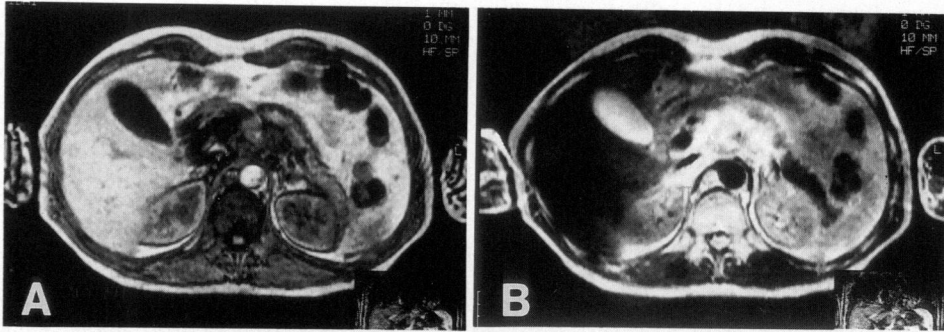


Fig. 9 MR imaging of hepatocellular carcinoma.

A. T1-weighted image by IR method (TR; 1500 ms, TI; 500 ms, TE; 18 ms)

B. T2-weighted image by SE method (TR; 2000 ms, TE; 90 ms)

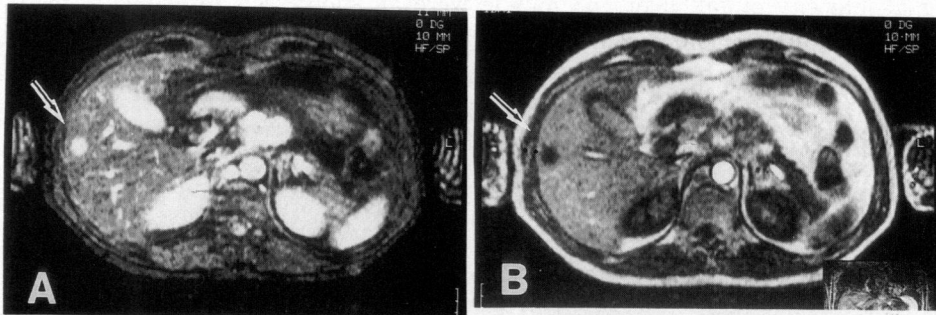


Fig. 10 MR imaging of hepatocellular carcinoma (Fig. 9) by STIR method.

A. TR; 1000 ms, TI; 100 ms, TE; 18 ms

B. TR; 1000 ms, TI; 300 ms, TE; 18 ms

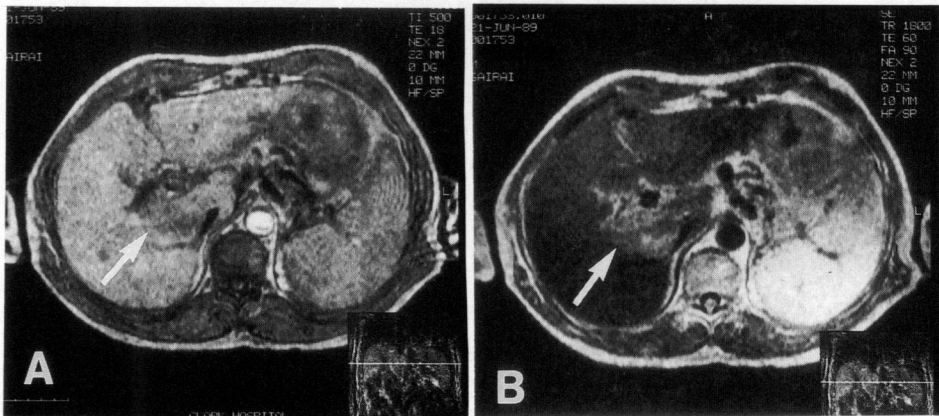


Fig. 11 MR imaging of cholangiocellular carcinoma.

A. T1-weighted image by IR method (TR; 1500 ms, TI; 500 ms, TE; 18 ms)

B. T2-weighted image by SE method (TR; 1800 ms, TE; 60 ms)

GS with T1 values and thus making the best use of the contrast resolution of MRI.

In 1987, Bydder *et al.* reported that a higher tumor contrast could be obtained after suppression of the signal intensity of fat by shortening the inversion time of the IR method, that is one of the common pulse sequence^(2,3). This was the short inversion time inversion recovery (STIR) method. The advantages of this method were ascertained by subsequent studies visualizing various organs, using medium- and high-magnetic-field MRI^(4,8,13,15). On the other hand, in Japan, Ikehira (1984) reported the usefulness of imaging using TI of 100 and 300 ms, although they did not refer this with the term STIR⁽¹⁷⁾.

In the present study, examination of phantoms by the STIR method (Fig. 4) revealed that the signal intensity of fat and liver are suppressed at a TI of 100 ms, and that tumors having high T1 values show a high signal. However, at TI of 150 ms or higher, a certain T1 value which suppressed the signal intensity to the greatest extent was found for each TI (fat at a TI of 100 ms, liver at 150 ms, muscle at 200 ms). This finding led us to consider that the choice of TI alters the signal intensity of each organ, providing characteristic images (Fig. 7). On the other hand, using both long TIIR (Fig. 3A) and medium TIIR (Fig. 3B), the peak signal intensity was obtained at a T1 value of 200 ms (corresponding to normal liver), and the GS value decreased, resulting in a low signal at a higher or lower T1 values. Since the contrast with the tumor was greater in the medium TIIR than in the long TIIR (Fig. 3A and 3B), the former method was expected to provide a higher tumor contrast.

In actual clinical application, T1- and T2-WI using low-magnetic-field MRI generally results in a lower signal intensity of the liver in comparison with that of the spleen, and therefore, it is often difficult to identify the tumor in cases of primary liver cancer (Figs. 8 and 9). Among the patients with hepatic tumors examined in the present study, hepatocellular carcinoma was identified in 22 out of 31 patients (37/58 nodules, 64%), cholangiocellular carcinoma in 3 out of 5 (3/6 nodules, 50%), metastatic liver cancer in 55 out of 68 (111/143 nodules, 78%), hepatic hemangioma in 32 out of 36 (41/47 nodules, 87%) and hepatic cyst in 8 out of 8 (100%). On the other hand, by STIR (TI=100 ms), the corresponding rate was 30/31 (54/58 nodules, 93%) for hepatocellular carcinoma, 5/5 (6/6 nodules, 100%) for cholangiocellular carcinoma, 66/68 (139/143 nodules, 97%) for metastatic liver cancer, 36/36 (47/47 nodules, 100%) for hepatic hemangioma and 8/8 (100%) for hepatic cysts (Table 1).

These findings indicate that STIR is highly useful for the detection of tumors. In particular, screening by this method using a TI of 50~100 ms provided very clear images of each tumor, since the signal intensity of fat, liver and

Table 1 *Detective ratio of Hepatic Tumors.*

	T1 & T2 weighted image (nodules %)	STIR image (nodules %)
Hepatocellular carcinoma	22/31 (37/58 : 64%)	30/31 (54/58 : 93%)
Cholangiocellular carcinoma	3/5 (3/6 : 50%)	5/5 (6/6 : 100%)
Metastasis	55/68 (111/143 : 78%)	66/68 (139/143 : 97%)
Hemangioma	32/36 (41/47 : 87%)	36/36 (47/47 : 100%)
Cyst	8/8 (8/8 : 100%)	8/8 (8/8 : 100%)

muscle were maximally suppressed (Fig. 4A). This was consistent with the concept of unwanted tissue signal suppression (UTSS) proposed by Lehmann, *et al.* in 1989⁽¹²⁾.

Therefore, in low-magnetic-field MRI for hepatic tumors, the use of STIR (TI=50~100 ms) is significant as a screening method. Qualitative diagnosis of such tumors seems to require T1- and T2-WI and STIR images obtained under various other conditions.

ACKNOWLEDGMENT

We thank Ms Itagaki for her technical assistance at Clark Hospital.

This work was supported in part by the Grant-in-Aid for Cancer Research (2-15) from the Ministry of Health and Welfare.

REFERENCE

1. BORKOWSKY, G. P., BUONOCORE, E., GEORGE, C. R., GO, R. T., O'DONOVAN, P. B. and MEANEY, T. F.: **J. Comput. Assist. Tomogr.** **7**, 768-774 (1983).
2. BYDDER, G. M. and YOUNG, I. R.: **J. Comput. Assist. Tomogr.** **9**, 659-675 (1985).
3. BYDDER, G. M., STEINER, R. E., BLUMGART, L. H., KHENIA, H. and YOUNG, I. R.: **J. Comput. Assist. Tomogr.** **9**, 1084-1089 (1985).
4. DOUSSET, M., WEISSLEDER, R., HENDRICK, R. E., STARK, D. D., CHRISTIAN, J. F., ELIZONDO, G., HAHN, P. F., SAINI, S. and FERRUCCI, J. T.: **Radiology** **171**, 327-333 (1989).
5. DOYLE, F. H., PENNOCH, J. M., BANK, L. M., MACDONNELL, M. J., BYDDER, G. M., STEINER, R. E., YOUNG, I. R., CLARKE, G. J., PASMORE, T. and GILDERDALE, D. J.: **A J R** **138**, 193-200 (1982).
6. DROEGE, R. T., WIENER, S. N. and RZESZOTARSKI, M. S.: **Radiology** **153**, 419-421 (1984).
7. DROEGE, R. T., WIENER, S. N. and RZESZOTARSKI, M. S.: **Radiology** **153**, 425-433 (1984).
8. DWYER, A. J., FRANK, J. A., SANK, V. J., REINIG, J. W., HICKEY, J. W. and DOPPMAN, J. L.: **Radiology** **168**, 827-836 (1988).

9. EBARA, M., OHTO, M., WATANABE, Y., KIMURA, K., SAISHO, H., TSUCHIYA, Y., OKUDA, K., ARIMIZU, N., KONDO, F., IKEHIRA, F., FUKUDA, N. and TATENO, Y.: **Radiology** **159**, 371-377 (1986).
10. IKEHIRA, H., FUKUDA, N., TATENO, Y., ENDO, M., MATSUMOTO, T., IINUMA, T. and EBARA, M.: **Kakuigaku** **21**, 1277-1283 (1984).
11. ITOH, K., NISHIMURA, K., TOGASHI, K., FUJISAWA, I., NOMA, S., MINAMI, S., SAGOH, T., NAKANO, Y., ITOH, H., MORI, K., OZAWA, K. and TORIZUKA, K.: **Radiology** **164**, 21-25 (1987).
12. LEHMANN, B., FANUCCI, E., GIGLI, F., UHLENBROCK, D. and BARTOLOZZI, C.: **J. Comput. Assist. Tomogr.** **13**, 650-655 (1987).
13. MORAN, P. R., KUMAR, N. G. and KARSTAEDT, N.: **Magn. Reson. Imaging** **4**, 229-235 (1986).
14. OHTOMO, K., ITAI, Y., FURUI, S., YASHIRO, N., YOSHIKAWA, K. and IIO, M.: **Radiology** **155**, 421-423 (1985).
15. SHUMAN, W. P., BARON, R. L., PETERS, M. J. and TAZIOLI, P. K.: **A J R** **152**, 853-859 (1989).
16. STARK, D. D., WITTENBERG, J., BUTCH, R. J. and FERRUCCI, J. T.: **Radiology** **165**, 399-406 (1987).
17. WATANABE, Y., EBARA, M., OHTO, M., YOSHIKAWA, M., SUGIURA, N., KIMURA, K., SAISHO, H., TSUCHIYA, Y. and OKUDA, K.: **Jpn. J. Gastroenterol.** **83**, 2550-2562 (1986).